CSMA 2026
17ème Colloque National en Calcul des Structures
18-22 mai 2026, Presqu'île de Giens (Var)

Muscle Fiber Characterization based on OCT: Towards Multiscale Muscle Modeling

A. Zaouali[1], MC. Ho Ba Tho[1] , O. Trabelsi[1]

[1] *Université de technologie de Compiègne, CNRS, Biomechanics and Bioengineering, France , aicha.zaouali@utc.fr ,hobatho@utc.fr , olfa.trabelsi@utc.fr*

Abstract — This study aims to characterize the morphological microstructure of the muscle in order to develop a multiscale Finite Element Model. The microstructure (Extracellular Matrix, fiber types (fast and slow twitch)) are assessed with Optical Coherence Tomography (OCT) aquisition coupled with mechanical tests. Four fiber-types were identified and quantified for the first time using OCT technique. The integration of microscale measurements into macroscale constitutive descriptions represents a key step toward consistent multiscale modeling.
Keywords — Fiber-type muscle, OCT characterization, multiscale modeling.

1. Introduction

Skeletal muscles generate movement through contraction and relaxation and are well organized in a hierarchical multiscale structure. The morphology begins from the sarcomere which is the contractile unit composed of myocytes (actin and myosin filaments). These myocytes form myofibers which are grouped in fascicles. Each fascicle contains several types of fibers : type I and type II fibers. Type I (slow-twitch) fibers are fatigue-resistant fibers in the opposite, Type II (fast-twitch) fibers contract quickly with high force but fatigue rapidly. In that context it is important to consider different types of fibers with the extracellular-matrix (ECM) environment for a better comprehension of the macroscopic behavior of the muscle. This will allow to develop a multiscale Finite Element Model based on microscale experimental data.

The literature review provides morphological data of different types of fibers for muscles from histological assessment [1-2]. Diameter values of fiber type I (slow-twitch) is 43.1± 2.4 µm. Four type II (IIA, IID/X, IIB) fibers were identified and the range of the diameter values vary from 45.2± 0.7µm to 75.5± 1.2µm. Cross Section Area (CSA) values of fiber type I is 1460±165 µm². Range of CSA values for type II vary from1605±50 µm² to 4478±140 µm². Concerning the values of fiber type II percentage, typical values were found to be 96% to 100%. According to the literature review [3], multiscale modeling geometries have typically been reconstructed from histological cross-sections.

The originality of the present study is to assess the morphological data of different type of fibers from Optical Coherence Tomography (OCT) acquisition coupled with mechanical testing in order to develop multiscale finite element models. Furthermore, the evolution of strain fields under stretch with fiber-type architecture and ECM organization in the muscle can be quantified. The different fiber-type and their percentage, ECM connectivity and local 3D geometry model will allow to determine the microstructural organization and their contribution in the macroscopic mechanical behavior of the muscle. These are of importance to reach the biofidelity of the multiscale model of the muscle.

2. Materials

2.1 Experimental OCT data

Muscle data are obtained from previous studies performed with OCT coupled with mechanical testing (Escobar et al.2024 [4]) (Fig.1). Two types of Wistar rat muscles have been investigated (EDL and the soleus). The EDL muscle contains about 90% type II (fast-twitch) fibers, and the soleus about 75% of type I (slow-twitch). The uniaxial tensile protocol with five stretch levels (5%, 8%, 11%, 14%, 17%) was applied, acquiring an OCT volume at each step after 20 min of relaxation, generating strain-dependent 3D datasets. Imaging used a Thorlabs OCT-TEL220C1.

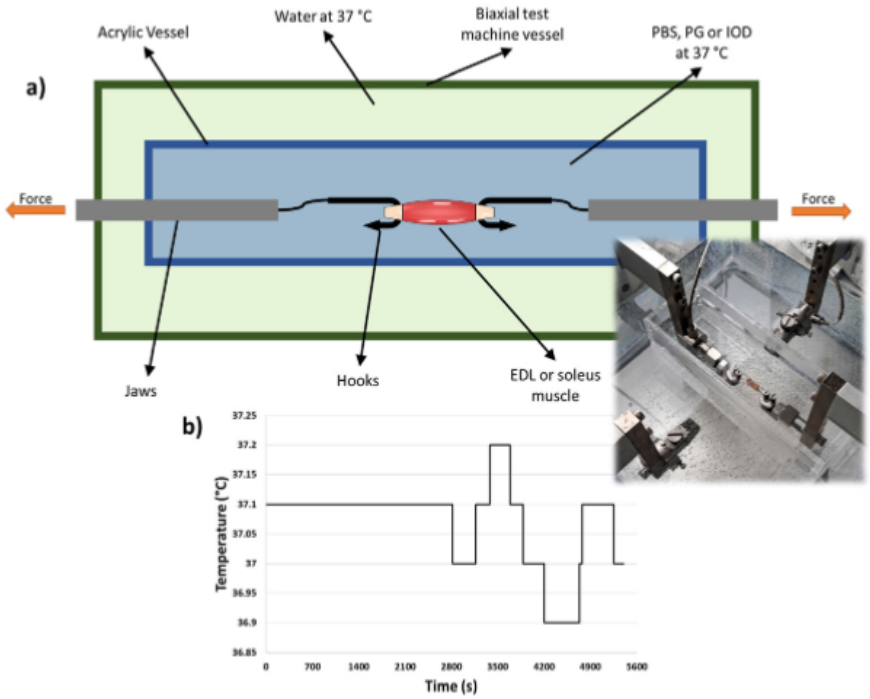

Figure 1 – **(a)** Top view of the uniaxial tensile testing setup. **(b)** Experiments were conducted at 37 ± 0.1 °C with muscles immersed in PBS or contrast agent. [4]

The datasets consist of volumetric OCT images of EDL muscle in TIFF format, enabling detailed microstructural analysis. For the present study, only one EDL muscle has been used for the morphological data assessment.

3. Methods

3.1 Data processing

3D OCT volume was available at each deformation level (5%, 8%, 11%, 14%, 17% strain) after relaxation. Volumes were provided in TIFF format (voxel size :1000 × 300 × 440 pixels equivalent : 5000 µm × 1500µm × 1078µm).

A multi-step filtering pipeline was then applied to enhance structural clarity. Bit-depth conversion (16-bit/float to 8-bit) standardized dynamic range, followed by Gaussian blurring (radius 1.5 px) and mean

filtering (radius 1 px) to attenuate high-frequency noise. Local artifacts were reduced via a minimum filter (radius 2 px). Finally, image sharpness was improved using a three-step unsharp mask (radius 1 px; weights 0.7, 0.9, 0.7) . This workflow produced denoised, contrast-enhanced OCT stacks suitable for segmentation and quantitative microstructural analysis, as shown in Fig. 2.

Figure 2 – Effect of the processing pipeline on OCT image quality (a) original, (b) after filtering.

Following processing, a 3D OCT representative volume element (RVE) (100 × 100 × 220 pixels) or 500µm x 500µm x539µm was extracted from the central region of each OCT dataset stretching level, as shown in Fig. 3. These coordinates were selected to avoid boundary artifacts and to isolate a stable portion of the muscle where fiber trajectories remain uniform. This 3D OCT RVE contains about 100 fibers which is higher compared to the literature [3]. In fact, it is important to ensure a significant number fibers, as boundaries will be affected by the stretching mechanical testing.

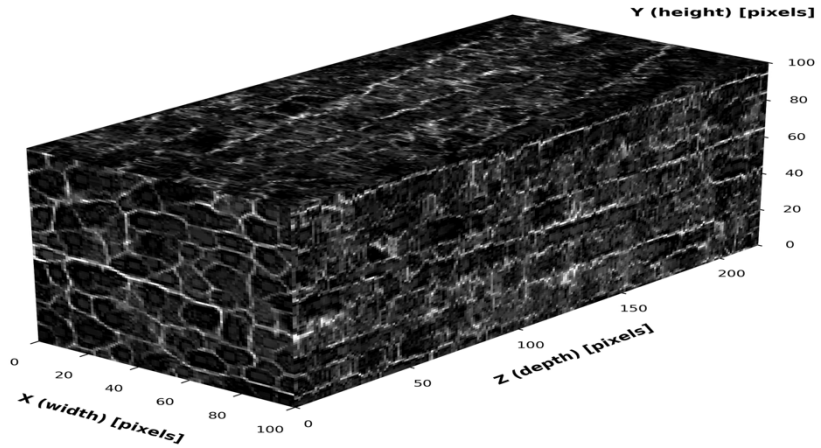

Figure 3 – 3D OCT RVE showing longitudinal and transverse muscle microstructure.
(X (500µm), Y (500µm), Z(539µm)

3.2 Segmentation

Segmentation of the 3D OCT RVE was performed using a semi-manual workflow combining threshold-based detection and detailed slice-level refinement. The 3D OCT RVE (100 × 100 × 220 pixels) was decomposed into 220 depth-resolved slices in ImageJ and imported into Mimics in non-DICOM format. An intensity threshold (79–255) was applied to enhance the visibility of the extracellular matrix (ECM), which appears as the brightest component in the OCT images. This produced an initial ECM mask that was subsequently refined manually on a slice-by-slice basis to remove speckle noise and correct incomplete or misleading contours. After manual cleanup, the slices were reconstructed into 3D, and a Boolean mask operation was applied to isolate the muscle fiber structure as shown in Fig. 4. This procedure yielded clean ECM boundaries and accurate fiber geometries in both orientations, enabling reliable microstructural and strain-dependent analyses.

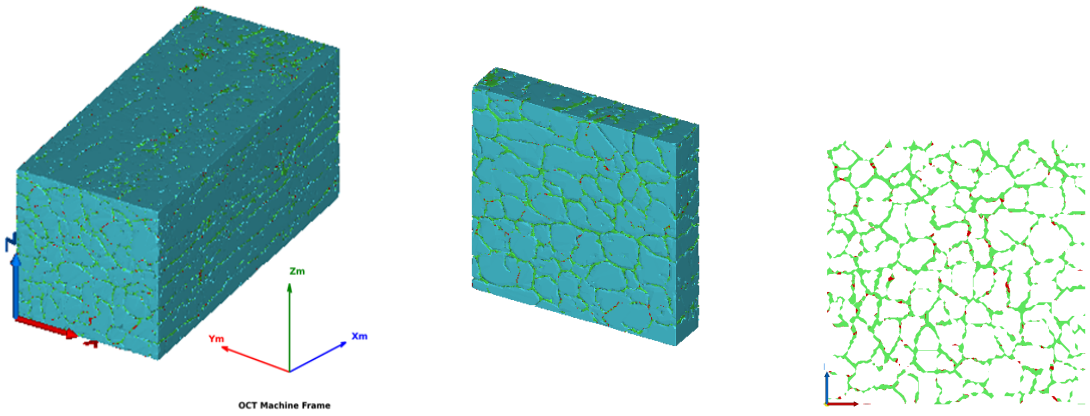

(a) (b) (c)

Figure 4 – **a)** 3D reconstruction of the extracted OCT sub-volume. **b)** Segmentation result from a 20-slice subset.**c)** ECM-only mask in a transverse section

3.3 Morphologic parameters calculation

Cross-sectional areas (CSA) were quantified using Mimics software (Materialise NV, Belgium) by manually outlining the ECM-based contours. In order to quantify the error of estimation of CSA, a subset of fibers was also evaluated using ImageJ software which used automated threshold-based CSA detection. This allows to compare both methods. Additionally, repeated manual measurements were performed on selected fibers to quantify operator repeatability across the dataset.This combined approach allows the CSA global error quantification. Then, Diameter fibers were calculated assuming their circularity in agreement with literature [1,2,4,5].

3.4. Statistical Analysis

K-Means clustering (k = 4) was applied to the diameter fibers and CSA data at all stretch levels. The choice of 4 clusters is based on the assumption that we are able to differentiate 4 types of fibers as mentioned in the literature review [1,2]. One-way ANOVA was used to evaluate whether fiber diameter and CSA varied across stretch levels within each cluster, using the F-statistic to determine significance, with $p < 0.05$. Both K-means clustering and one-way ANOVA were implemented in Python 3.10.11 using the libraries pandas, Matplotlib, scikit-learn (K-Means), NumPy, and SciPy (f_oneway).

3.5. Multiscale model of the muscle

By combining global and local morphometric data across stretch levels, multiscale finite element model can be obtained based on STL files generated from segmentation, integrating multiscle data derived from OCT. Thanks to the experimental data available, passive mechanical properties of different type of fibers could be assessed. These new knowledge will be used to describe appropriately the skeletal muscle with different composition of slow, fast fibers for the multiscale modelling.

4. Results and Discussion

Segmentation results for the same transverse slice across stretch levels are illustrated in Fig.5. We can observe an increase of fibers for the different stretching levels : 118 fibers at 5%, 124 at 14%, and 130 at 17% stretch. The increase reflects fiber alignment under loading, allowing additional fibers to enter the fixed 100 × 100-pixel window.

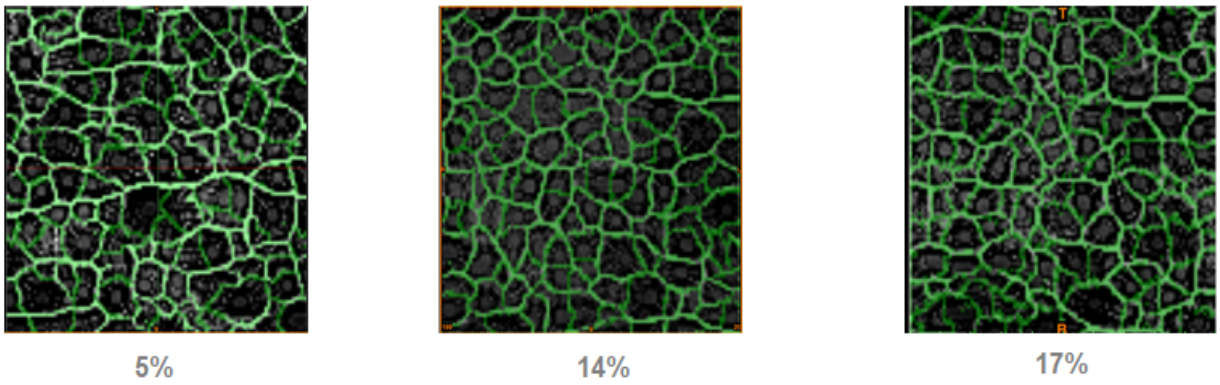

Figure 5 – Segmented transverse OCT slices at 5%, 14%, and 17% stretch showing ECM-defined fiber boundaries within the 100 × 100-pixel analysis window

CSA values were extracted from the segmented contours, and circular-equivalent diameters were calculated for comparison with literature. Diameter distributions (Fig. 6) showed mean values of 48.2±12.28µm (5%), 47.7±11.26µm (14%), and 46.39±12.03µm (17%), with a small, consistent reduction as stretch increased. This is consistent with transverse contraction during axial loading.

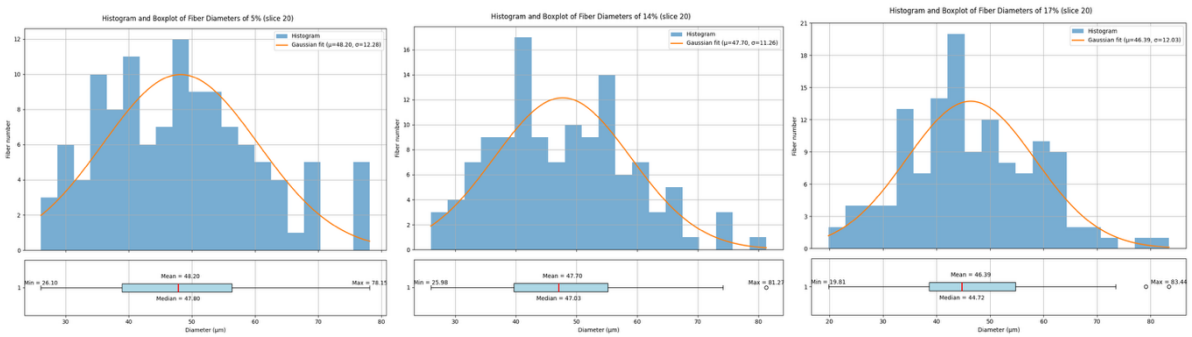

Figure 6 – Histograms and boxplots of fiber diameters at 5%, 14%, and 17% stretch from Slice 20

CSA distributions displayed a similar decrease with stretch, with mean values of 1942.15± 987.23µm² (5%), 1885.53±890.96µm² (14%), and 1802.76±923.47µm² (17%). The reduction in CSA further supports the expected geometric response of fibers under tensile deformation.
The relative error of CSA measurements with both methods (manual versus automatic) is 27 ± 12 % . Repeated manual assessments give a variability of 112.75 ± 87 µm², corresponding approximatively to 15% of error measurement.

The results of K-Means clustering (k = 4) show comparable values obtained in the literature review (Table 1). This implies that the four clusters correspond to Type I, Type IIA, Type IID/X, and Type IIB fibers, from the smallest to the largest. Values of the muscle with 5% stretch data, representing the initial state of the muscle, are compared with data reported in the literature (**Table 1**).

Table 1 – Comparison OCT-Based EDL Muscle Microstructure at 5% and histological data performed on EDL muscle [2]

		Cluster 1 (Type I slow)	Cluster 2 (Type II A)	Cluster 3 (Type IID/X)	Cluster 4 (Type IIB)
CSA (µm²)	OCT 5%	1059 ± 262	1966 ± 254	2854 ± 267	4177 ± 475
	Histology	1460 ± 165	1605 ± 50	2215 ± 78	4478 ± 140
Diameter Ø (µm)	OCT 5%	32.8 ± 3.3	43.7 ± 3.6	55.5 ± 3.8	69.9 ± 5.5
	Histology	43.1± 2.4	45.2± 0.7	53.0± 0.9	75.5 ± 1.2

Values of diameters of fiber type II (fast) are in agreement with histological data. The relative difference of diameters of fiber type I (slow) and CSA values between OCT and histological data is 24% and 21% respectively. It should be noted that the histology and OCT methods do not have the same protocol of muscle preservation and it affects the fiber and its ECM environment.

The resulting cluster-wise fiber CSA, diameter, and fiber-type percentage at 5%, 14%, and 17% stretch levels are summarized in **Table 2**.

The fiber type II (fast twitch) percentage was found to be about 78% which is consistent and relevant as it is expected [1,2]. This comforts the ability of OCT technique to characterise different fiber type.

Table 2 – OCT-Based EDL Muscle Microstructure at 5%, 14%, and 17% Stretch Levels

		Cluster 1 (Type I slow)	Cluster 2 (Type IIA fast)	Cluster 3 (Type IID/X fast)	Cluster 4 (Type IIB fast)
CSA (µm²)	5%	1059 ± 262	1966 ± 254	2854 ± 267	4177 ± 475
	14%	949 ± 211	1623 ± 250	2544 ± 301	3878 ± 605
	17%	951 ± 285	1780 ± 258	2844 ± 280	4373 ± 813
Diameter Ø (µm)	5%	32.8 ± 3.3	43.7 ± 3.6	55.5 ± 3.8	69.9 ± 5.5
	14%	33.4 ± 3.5	43.7± 3.1	55.2± 3.8	68.5 ± 5.5
	17%	30.4 ± 4.4	42.1 ± 2.8	51.6 ± 2.7	63.4 ± 6.3
Persentage (%)	5%	22	34.8	30.6	12.7
	14%	21.8	36.3	31.5	10.5
	17%	20.8	35.4	22.3	21.5

We can observe that the values seemed to decrease from 5% to 17% stretch levels for all the clusters. Results of one-way ANOVA analyses show that some diameter fiber values are decreasing significantly.

Globally, for all the clusters, the diameter fiber, CSA and the percentage of fiber Type I and fiber Type II (IIA+IID/X+IIB) are statiscally significantly decreasing from 5% to 14% or from 5% to 17% stretch level.

The variation in fiber type distribution with increasing stretching levels confirms that tissue mechanical properties are stretch-dependent.

By incorporating experimentally observed stretch-dependent microstructural changes, nonlinear and anisotropic constitutive models can be developed, significantly improving the physiological relevance and predictive capability of multiscale skeletal muscle models. The integration of microscale measurements (fiber CSA, orientation, local strain) into macroscale constitutive descriptions represents a key step toward consistent multiscale modeling. Figure 7 illustrates the preliminary multiscale finite element model of the muscle derived from OCT stl files (Figures 3 and 4).

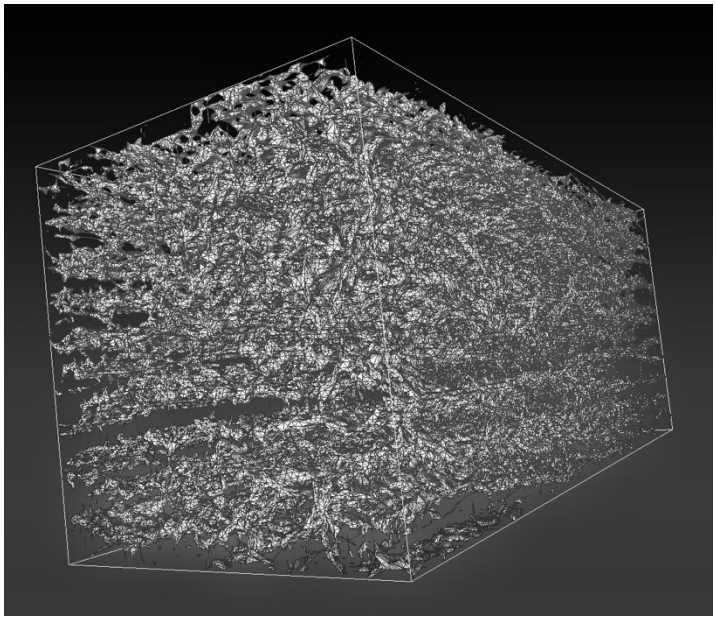

Figure 7. Finite element reconstruction of the ECM from OCT RVE.

5. Conclusions and Perspectives

In this study, morphometric fiber parameters were analyzed on one section of a 3D OCT RVE, at different stretch levels. Even the measurements were performed on one section of the 3D OCT RVE, results showed that the classification of fiber types (Type I, Type IIA, IID/X, and IIB) from OCT data was possible. This represents an original contribution to muscle microstructure characterization in its natural environment compared to histological measurements and the development of the multiscale finite element model.

Future work will focus on expanding the dataset by including intermediate stretch levels (8%, 11%) and performing multiple sections of 3D OCT RVE to improve statistical robustness, as well as incorporating additional EDL muscle samples.

Extending the analysis to other muscles, such as the Soleus, which contains a higher proportion of Type I fibers, will further enhance fiber-type characterization.

References

[1] C. M. Eng, L. H. Smallwood, M. P. Rainiero, M. Lahey, S. R. Ward, & R. L. Lieber (2008). Scaling of muscle architecture and fiber types in the rat hindlimb. *Journal of Experimental Biology, 211*(14), 2336–2345.

[2] B. Delp, Y. Duan. *Composition and fiber cross-sectional areas of rat skeletal musculature***,** Journal of Morphology, Wiley, pp. 1–N, 1996

[3] A. Loumeaud, P. Pouletaut, S. F. Bensamoun, D. George, & S. Chatelin (2024). *Multiscale mechanical modeling of skeletal muscle: A systemic review of the literature*. Journal of Medical and Biological Engineering, 44, 337–356.

[4] J. F. Escobar-Huertas, J. J. Vaca-González, D. A. Garzón-Alvarado, & O. Trabelsi (2024). *Effect of iodixanol and propylene glycol as clearing agents in extensor digitorum longus and soleus muscles: Mechanical and morphological characterization using the optical coherence tomography technique*. Biomaterials Science, 12, 5295–5310.

[5] M. Maillet, M. Kammoun, S. Avril, M.-C. Ho Ba Tho, & O. Trabelsi(2023). *Non-destructive characterization of skeletal muscle extracellular matrix morphology by combining optical coherence tomography (OCT) imaging with tissue clearing*. Annals of Biomedical Engineering, 51, 2323–2336.